JOURNAL OF THERMOPHYSICS AND HEAT TRANSFER
Vol. 14, No. 4, October–December 2000

Potential Energies and Collision Integrals for Interactions of Carbon and Nitrogen Atoms

James R. Stallcop* and Harry Partridge†
NASA Ames Research Center, Moffett Field, California 94035-1000
Atul Pradhan‡
SVG Lithography, Wilton, Connecticut 06897
and
Eugene Levin§
Eloret Corporation, Moffett Field, California 94035-1000

Potential energies for C_2 and CN are calculated by a configuration interaction method for those states for which the molecule dissociates into ground state atoms. The potential energy curves are shown graphically; parameters determined from the potential energy wells are tabulated and compared with the corresponding data available from measurements. The potential energies of the $^7\Sigma_u^+$ and $A'^5\Sigma_g^+$ states of N_2 are computed from very accurate state-of-the-art molecular structure calculations and improved using the results of spectroscopic measurements, respectively. Transport cross sections are tabulated for a broad range of collision energies. Collision integrals are determined from the cross sections; the C–C and C–N results are tabulated for temperatures in the range 300–30,000 K. The improved collision integrals for N–N interactions differ from the corresponding results of an existing tabulation by a small insignificant amount. The scattering results are used to validate simple methods for estimating collision integrals and to examine the diffusion, viscosity, and thermal diffusion in a gas composed of carbon and nitrogen atoms.

Nomenclature

a_0 = Bohr radius, 5.291772×10^{-9} cm
C_n = long-range coefficient, $E_h a_0^n$
D = coefficient of diffusion, cm^2/s
D_e = potential energy well depth, eV
D^* = reduced coefficient of diffusion
E = collision energy, E_h
E_h = hartree, 27.211396 eV
g_i = degeneracy factor for ith state
m = mass of the atom, amu
p = pressure, atm
Q = transport cross section, a_0^2
r = separation distance, a_0
r_e = equilibrium separation distance, a_0
r_m = position of maximum of the potential energy, a_0
r_0 = Lennard–Jones separation distance [e.g., $V(r_0) = 0$], a_0
T = temperature, K
T_e = transition energy, eV
V_e = effective atom–atom interaction energy, E_h
V_i = potential energy for the ith molecular state, E_h
V_q = potential energy for quintet state of N_2, E_h
V_{SR} = short-range repulsive energy, E_h
V_s = potential energy for septet state of N_2, E_h
α = thermal diffusion factor
η = coefficient of viscosity, gm/(cm s)
η^* = reduced coefficient of viscosity
κ = Boltzmann constant
σ = length scale factor, a_0
Ω = collision integral, $Å^2$
ω_e = vibrational frequency, cm^{-1}

Received 25 October 1999; revision received 14 February 2000; accepted for publication 14 February 2000.

*Physicist, Computational Chemistry Branch, Space Technology Division, M/S 230-3.
†Chemist, Computational Chemistry Branch, Space Technology Division, M/S 230-3.
‡Senior Staff Engineer, Advanced Programs.
§Senior Research Scientist, Thermosciences Institute, M/S 230-3.

I. Introduction

THE potential energy curves and transport properties for atom–atom interactions are needed for studies of gases and plasmas such as those of the high-temperature environment for aeroentry into planetary atmospheres, for the study of stellar atmospheres, and for the manufacturing or preparation of certain electronic devices.[1] The interactions of carbon and nitrogen are important for studies of space vehicles with carbonaceous heat shields. Furthermore, carbon plays an important role in reducing radiative and conductive heating of such space vehicles.[2] Nitrogen is the major component of air; hence, accurate transport properties for nitrogen interactions are required for a proper analysis of high-altitude flight and certain atmospheric phenomena.

With the exception of interactions involving rare-gas atoms, atom–atom transport properties cannot be measured in the laboratory by the usual methods because of the difficulty of producing gases with a pure species concentration. The effective potential energies deduced from scattering measurements are not unique; hence, the transport properties obtained from interaction energies, which are constructed from experimentally deduced energies using additive and combining schemes, are not reliable. Commonly applied computer codes for the prediction of atom–atom transport data are based on inappropriate potential functions with parameters that are constructed from questionable empirical rules.

The diffusion and viscosity integrals have been calculated by Biolsi et al.[3] for C–C interactions at temperatures $\geq$1000 K. As pointed out,[3] however, there is a large uncertainty in their results arising from the uncertainty in the potential energy curves of excited states of C_2. The curves for many of the excited states were based on the results of early ab initio calculations[4]; moreover, unknown curves were estimated using valence-bond theory.

More recent advances in computer technology and computational methods for the determination of electronic structure, such as those described in Secs. II and III, allow an accurate determination of the potential energy curves for all separation distances of the collision

pair that are required for the calculation of transport properties. Furthermore, previous transport calculations[3] used potential energy functions that were fitted to measured data, which describe only a limited region around the well minimum, whereas the present scattering calculations use the actual potential energy curve for all separation distances. The elimination of the uncertainty arising from extrapolated repulsive energies is especially important for the determination of the scattering from the high-spin states that provide the major contribution to transport properties at high temperatures.

In the present work we determine complete sets of accurate potential energy curves of C_2 and CN; i.e., we consider all states that dissociate to ground state atoms. To ensure that accurate results are obtained, the potential energy curves are evaluated using a configuration-interaction method with a large one-electron basis set. This yields results of similar quality to our previous work on transport properties.[5–7] The potential energy curves for the two highest spin states of N_2, which provide the dominant contribution to N–N transport properties, are also considered in the present work. Here experimental data and the results of a high-level theoretical calculation are used to obtain our final potential energy curves.

The potential energy results have been applied to calculate transport cross sections, using methods that are based on a quantum mechanical formulation of the scattering. At low collision energies the scattering phase shifts were obtained from a numerical integration of the Schrödinger equation. Transport collision integrals obtained from the cross sections are tabulated for C–C and C–N interactions; the results for N–N are applied to test the accuracy of previous tabulations.[6] The collision integrals are applied to study the behavior of transport properties for various concentrations of carbon and nitrogen atoms.

In general, the accurate theoretical determination of transport properties is very laborious because it requires a complete set of interaction energies corresponding to all possible paths available to the collision. Nevertheless, sets of accurate atom–atom collision integrals are required to validate simpler methods that predict transport data with less effort.

For interactions in which one of the collision partners is a rare-gas atom such as helium, the computational effort is relatively small, and studies are underway to develop Aufbau procedures from which the transport properties of a complex X–X interaction can be inferred from the properties of the simplier He–He and He–X interactions. The present collision integrals and the results of other accurate calculations are used to test the Aufbau method for consecutive members of the first row of the periodic chart.

II. C–C and C–N Interaction Energies

The accuracy of theoretical interaction energies can be judged from convergence studies of ab initio calculations and comparisons with the results of spectroscopic and other experimental measurements. The dissociation energies of the ground states of C_2 and CN have been measured accurately. The laser-induced fluorescence study of Urdahl et al.[8] and the measurements of Huang et al.[9] yield values 6.411 ± 0.02 eV and 7.866 ± 0.02 eV for the potential well depths D_e of the ground states of C_2 and CN, respectively. Pradhan et al.[10] have combined various large one-electron basis sets with large-scale configuration interaction (CI) techniques to study the ground states of C_2 and CN; their results agree well with these measured results (to within about the experimental uncertainty) and with the experimentally determined equilibrium separation distance r_e and vibrational frequency ω_e. Additional convergence studies by Peterson,[11] Partridge and Bauschlicher,[12] and Peterson et al.[13] on C_2 have been reported. These studies also yield results that agreed well with experiment. Thus it is possible to obtain highly accurate potential energy curves from ab initio electronic structure calculations for the preceding interactions.

An approach that is less expensive than the highest-level methods of the preceding convergence studies but near in quality should be adequate for our scattering calculations because transport properties are relatively insensitive to small variations in the interaction energy. Thus we performed multireference configuration-interaction (MRCI) calculations with orbitals optimized using complete active space self-consistent-field (CASSCF) orbitals. Internal contraction is used to keep the size of the calculations manageable. In the CASSCF calculations the $2p$ orbitals are active, whereas in the MRCI calculations both the $2s$ and $2p$ orbitals are active for a total of eight active electrons for C_2 and a total of nine active electrons for CN. We use the augmented correlation-consistent polarized-valence quadruple-zeta (aug-cc-pVQZ) basis sets of Dunning and coworkers.[14–16] The effects of higher-order excitations are accounted for by using the multireference analog of the Davidson correction[17] (+Q). These calculations were carried out using the program package MOLPRO, as described in Ref. 18.

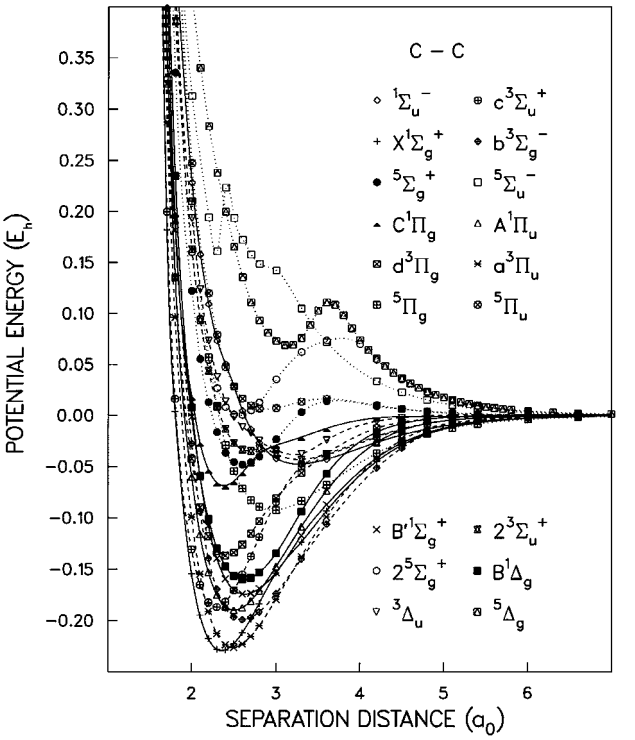

Fig. 1 C_2 potential energy curves; the ——, - - - -, and · · · · curves are obtained from spline fits to the ab initio data points for singlet, triplet, and quintet states, respectively.

The potential energy curves $V_i(r)$ obtained from the present ab initio calculations are shown for C_2 and CN in Figs. 1 and 2, respectively. Parameters describing the potential minima from the present calculations are compared with the corresponding measured results for C_2 (Refs. 8 and 19) and CN in Tables 1 and 2, respectively. Unless otherwise noted, the values of r_e, ω_e, and the transition energy T_e that are deduced from spectroscopic measurements are taken from Ref. 20.

The ab initio results are extended to larger values of r, using long-range expansions of the interaction energies. For scattering at very low collision energies E, the spin-orbit interactions must be taken into account for interactions involving carbon; however, because we are primarily interested in the transport properties for temperatures T above 300 K, we use the Russell–Saunders L-S coupling scheme employed for the ab initio calculations. The construction of the potential energies for low E is discussed in Sec. IV. The carbon atom has a quadrupole moment; hence, the leading coefficient is C_5 for certain states of C_2. The values of these coefficients have been determined from the formulation of Chang[21] using the results of a relativistic Hartree–Dirac calculation.[22] The value of C_5 is found to be $-14.41\ E_h a_0^5$ for $C^1\Pi_g$, $a^3\Pi_u$, and $^5\Pi_g$ states; $3.63\ E_h a_0^5$ for $B^1\Delta_g$, $^3\Pi_u$, and $^5\Delta_g$ states; and $21.69\ E_h a_0^5$ for $B'^1\Sigma_g^+$, $(2)^3\Sigma_u^+$, and $(2)^5\Sigma_g^+$ states. The value of C_5 vanishes for the remaining states that correspond to dissociation into ground state atoms.

Note from Fig. 1 that the $^5\Delta_g$ state, which yields one of the largest contributions to transport properties, interacts strongly (exhibits an avoided crossing) with another excited state. The V for this state at large r is constructed from a realistic van der Waals potential energy

Table 1 Potential energy parameters for states of C_2

State[a]	r_e	D_e	T_e	ω_e
$X^1\Sigma_g^+$	2.357	6.24	0	1844
Expt.	2.348	6.41[b]	0	1855
$A^1\Pi_u$	2.502	5.17	1.07	1596
Expt.	2.491	5.37	1.04	1608
$B'^1\Sigma_g^+$	2.629	4.75	1.49	1417
Expt.[c]	2.603	4.50	1.91	1424
$B^1\Delta_g$	2.614	4.36	1.88	1398
Expt.[c]	2.618	4.91	1.50	1407
$C^1\Pi_g$	2.382	1.87	4.37	1822
Expt.	2.372	2.16	4.25	1809
$^1\Sigma_u^-$	3.265	1.30	4.94	721
$a^3\Pi_u$	2.490	6.15	0.09	1600
Expt.	2.479	6.32	0.09	1641
$b^3\Sigma_g^-$	2.599	5.42	0.82	1448
Expt.	2.587	5.61	0.80	1470
$c^3\Sigma_u^+$	2.291	5.09	1.15	1995
Expt.	2.32	4.76	1.65	1962
$d^3\Pi_g$	2.321	3.72	2.52	1774
Expt.	2.393	3.93	2.48	1788
$(2)^3\Sigma_u^+$	3.272	1.18	5.06	784
$^3\Delta_u$	3.218	1.05	5.19	1000
$^5\Pi_g$	2.568	2.53	3.71	988
$(1)^5\Sigma_g^+$	2.600	1.32	4.92	1484
$(2)^5\Sigma_g^+$	2.560	——	6.23	1521
$^5\Pi_u$	2.248	——	6.40	890
$^5\Delta_g$	3.144	——	8.10	1523
$^5\Sigma_u^-$	2.250	——	10.55	——

[a]First and second row for each state contain values from theory and experiment, respectively.
[b]Ref. 8. [c]Ref. 19.

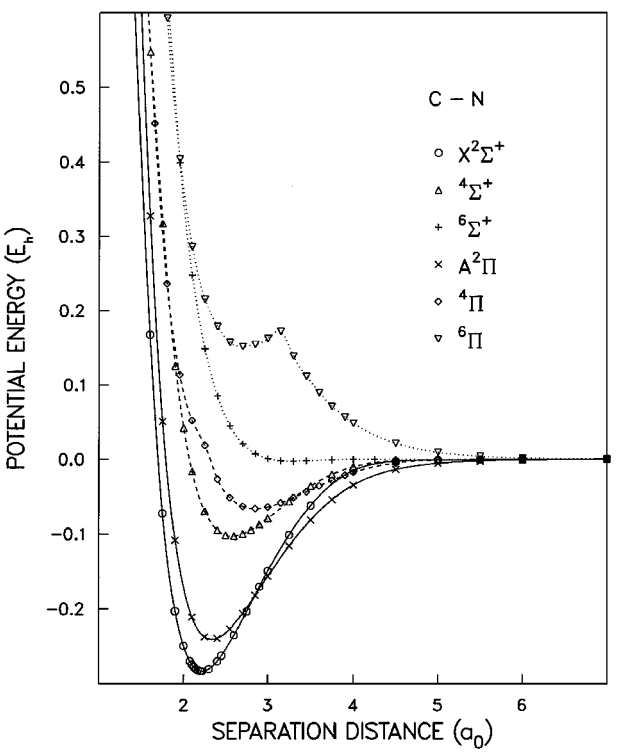

Fig. 2 CN potential energy curves: the ——, - - - -, and · · · · curves are spline fits to the ab initio data points for doublet, quartet, and sextet states, respectively.

Table 2 Potential energy parameters for states of CN

State[a]	r_e	D_e	T_e	ω_e
$X^2\Sigma^+$	2.222	7.71	0	2064
Expt.	2.214	7.87[b]	0	2067
$A^2\Pi$	2.338	6.57	1.14	1799
Expt.	2.330	6.72	1.15	1813
$^4\Sigma^+$	2.575	2.80	4.90	1310
$^4\Pi$	2.846	1.80	5.91	960
$^6\Sigma^+$	3.280	0.08	7.63	446
$^6\Pi$	2.693	——	11.84	1185

[a]First and second row for each state contain values from theory and experiment, respectively.
[b]Ref. 9.

function[23] using the ab initio data for the repulsion at smaller r and the long-range coefficients. The required higher-order dispersion coefficients C_n for $n \geq 8$ are approximated by the formulation of Starkshall and Gordon[24] using the calculated moments of Ref. 22.

III. N–N Interaction Energies

Bauschlicher and Partridge[25] have studied the convergence of r_e, D_e, and ω_e for the N_2 ground state using various high-level calculations. More recent studies[13] also find good agreement with measured values.[20] We have performed high-level calculations using the restricted coupled-cluster singles and doubles approach[26,27] including the effect of connected triples determined using perturbation theory[28,29] [RCCSD(T)] and large quintet-zeta (5Z) basis sets[14–16] to determine $V(r)$ for the $^7\Sigma_u^+$ state, which provides the major contribution to N–N transport properties. We have also included midpoint-centered bond functions[30] and applied the counterpoise method[31] to correct for basis set superposition error (BSSE) to ensure that the calculated energies are accurate, especially at large r.

The ab initio energy at large r is found to agree well with that obtained from a long-range expansion using the dispersion coefficients determined by Partridge et al.[32] Compared to the ab initio values of the potential energy $V_s(r)$ of Ref. 32, we obtain a lowering of the energies of the repulsive wall. The small percentage decrease for r less than about 4–5 a_0 can be neglected for transport calculations. For larger r a small rotation[33] of the linear curve of a semilog plot of the short-range repulsive energy $V_{SR}(r)$ vs r can be applied to fit the difference

$$V(r) - V_s(r) \approx -0.082(r - 4.4)V_{SR}^s(r) \quad (1)$$

the quantity $V_{SR}^s(r)$ is extracted from $V_s(r)$, using the method of Stallcop et al.[34] and the C_n of Ref. 32, to obtain the relation

$$\ell n V_{SR}^s(r) = 3.27 - 1.703r \quad (2)$$

The units of $V(r) - V_s(r)$ are E_h when r is expressed in a_0 in both Eqs. (1) and (2). The value of the separation distance r_0 for which the potential energy vanishes [i.e., $V(r_0) = 0$] is 6.436 a_0, which is smaller than the corresponding result for $V_s(r)$. Also consistent with the lower energies of Eq. (1), we find a deeper van der Waals potential energy well; the values of r_e and D_e from the present calculation are 7.20 a_0 and 3.64 meV, respectively.

To further improve on our previous potential results[6] for N–N interactions, $V_q(r)$ for the metastable $A'^5\Sigma_g^+$ state calculated by Partridge et al.[35] has been adjusted at small r to fit the inner potential energy well derived from spectroscopic experiments. The theoretical values of r_e and the minimum of the potential energy well of $V_q(r)$ are shifted by $\Delta r_e = -0.021$ a_0 and lowered by 60 meV, respectively, to conform with the results from the measurements of the Herman infrared bands[36] and T_e (Ref. 37). The repulsive wall at small r and the potential energy barrier at large r from the ab initio results are required to remain unchanged. The uncertainty in the results for the transport data that arises from joining the potential energy from the spectroscopic data to the calculated data according to the preceding criteria is small. Assuming that the ab initio asymmetry of the well is satisfactory, the adjustment of $V_q(r)$ outside the well region is readily accomplished with suitable functions that are

Table 3 Atom–atom transport cross sections[a]

	$\bar{Q}_1(E)$			$\bar{Q}_2(E)$			$\bar{Q}_3(E)$		
E	C–C	C–N	N–N	C–C	C–N	N–N	C–C	C–N	N–N
0.0001	467.23	369.35	325.44	373.53	289.82	244.53	547.83	419.29	367.97
0.0002	336.78	277.58	238.85	273.07	226.82	209.05	405.83	328.80	286.00
0.0003	292.80	246.69	188.09	232.61	185.67	169.10	345.48	288.99	237.38
0.0005	239.50	207.19	144.35	200.75	152.19	126.93	285.50	236.66	180.14
0.0007	208.70	179.20	123.13	171.06	143.08	106.45	249.39	205.37	150.44
0.0010	180.71	146.95	109.94	150.34	129.19	94.75	216.55	176.17	131.41
0.0015	157.21	116.98	100.18	128.62	106.77	83.46	186.70	147.58	115.88
0.0020	142.40	100.85	94.41	116.51	91.63	76.27	168.86	127.09	108.24
0.0030	123.56	87.54	82.90	101.57	75.66	69.72	145.98	106.76	96.98
0.0040	113.33	83.07	76.41	92.53	69.24	65.06	133.32	98.45	90.42
0.0050	107.58	76.30	72.80	86.96	64.20	60.99	126.09	90.17	85.49
0.0060	101.11	73.11	68.53	81.92	61.23	57.18	118.46	85.93	80.35
0.0070	99.01	70.77	66.86	78.83	59.15	54.36	115.26	82.82	77.88
0.0080	94.72	68.71	66.13	76.57	56.77	53.12	110.28	80.24	76.19
0.0090	91.35	66.89	63.59	73.01	55.70	51.40	106.42	78.13	73.58
0.0100	90.32	66.06	61.39	71.93	54.53	50.22	104.79	76.70	71.15
0.0150	80.58	66.39	58.09	64.45	52.56	46.69	93.49	76.15	66.68
0.0200	74.10	62.19	54.52	59.78	48.99	43.83	86.79	70.99	62.78
0.0300	65.44	53.16	50.01	52.41	42.61	40.64	77.37	61.16	57.86
0.0400	60.87	50.43	47.07	47.54	40.36	38.18	71.48	58.06	54.59
0.0500	56.81	48.16	44.21	45.21	38.37	36.57	66.50	55.41	51.81
0.0600	53.45	46.04	41.16	42.90	36.88	34.65	62.90	53.23	49.08
0.0700	50.50	44.61	39.24	40.91	35.72	33.16	59.84	51.69	46.91
0.0800	47.55	42.25	37.75	39.70	35.14	31.56	56.61	49.30	45.08
0.0900	44.74	40.20	36.18	38.47	34.38	30.64	53.92	47.59	43.33
0.1000	42.40	38.57	35.07	37.04	33.51	29.67	51.80	46.37	41.95
0.1500	33.23	32.01	29.87	31.38	29.10	26.69	42.94	40.13	36.24
0.2000	26.08	27.07	26.29	27.46	26.31	24.23	35.70	34.81	32.90
0.3000	18.59	19.17	22.04	20.46	21.13	20.67	27.35	27.49	27.97
0.5000	13.25	13.22	17.10	13.66	14.26	16.91	18.85	19.42	22.42
0.7000	11.16	10.86	14.23	11.00	11.30	14.61	15.18	15.42	19.25

[a]Energies and and cross sections are in units of E_h and a_0^2, respectively.

chosen to be symmetrical about the well minimum; e.g., the shift in r is obtained with

$$\Delta r = \Delta r_e \left(1 - \tanh\left\{(1/a)[(r - r_e)/(r_m - r_e)]^2\right\}\right) \qquad (3)$$

where r_m is the position of the barrier maximum and a is an adjustable parameter.

The theoretical van der Waals potential energies for both of the high-spin states of N_2 just discussed are extended to large r using the C_n of Ref. 32 and the method outlined in Sec. II for carbon interactions.

IV. Transport Cross Sections and Collision Integrals

The spin-orbit interaction is important[38] for transport cross sections for atoms with carbon as a collision partner at low E, but has a small effect at high E. The interaction energies at large r required for the spin-orbit coupled states could be constructed by a unitary transformation[39] using the L-S results for the $V_i(r)$ described in Sec. II. A discussion of the effects of fine structure on scattering is contained in Ref. 40. An accurate calculation of carbon transport at low T is, however, beyond the scope of the present investigation.

The symmetry effects of nuclear spin s on elastic scattering of identical atoms is small[41] at high E. The present scattering calculations are based on the high-T semiclassical scattering description for transport properties by Mason et al.[42]

The transport cross sections $Q_n^i(E)$ are determined from a quantum mechanical formulation[6] of the elastic scattering in the field of $V_i(r)$ for the ith molecular state. The phase shifts have been calculated at lower E from a numerical integration of the Schrödinger equation, using the method of Levin et al.[43] A semiclassical method[7,44] is applied to approximate the phase shifts at higher E above a threshold energy E_t, where the difference in the cross sections between the two methods is less than three units in the fourth significant figure.

The transport cross sections $\bar{Q}_n(E)$ are obtained from an average[42,45] of the $Q_n^i(E)$ for each state according to their degeneracies g_i. Carbon and oxygen have similar ground states (^3P); hence, the statistical weights listed for oxygen interactions in Ref. 45 are directly applicable to the interactions involving carbon of this work.

The calculated values of $\bar{Q}_n(E)$ are listed in Table 3. The values of $\bar{Q}_n(E)$ for C–C and C–N interactions are obtained using the $V_i(r)$ of Sec. II; the values for N–N interactions are obtained from the $V_i(r)$ of Sec. III for the high-spin states and the results for the lower ($X^1\Sigma_g^+$ and $A^3\Sigma_u^+$) states of Ref. 6, which were constructed from both theoretical and experimental data.

As in our previous atom–atom studies,[6] we find that the contribution to the transport data from the bound states that have been observed in spectroscopic experiments is relatively small. For example, the nine states that have spectroscopic labels in Table 1 contribute 30–36% to the $\bar{Q}_2$ listed in Table 3 for carbon interactions; similarly, the two spectroscopic states of CN listed in Table 2 contribute 19–29% to $\bar{Q}_2$ for C–N. The $X^1\Sigma_g^+$ and the $A^3\Sigma_u^+$ states of N_2 contribute 20–30% to $\bar{Q}_2$ for N–N. Because the major contribution comes from the higher lying states with the large values of g_i, the calculation of transport cross sections relies heavily on ab initio calculations for excited states.

The $\bar{Q}_n(E)$ are required for studies of gases or plasmas with certain severe nonequilibrium conditions. When a Maxwell–Boltzmann velocity distribution is valid, transport properties are obtained[46] from the collision integrals

$$\bar{\Omega}_{n,s}(T) = \frac{F(n,s)}{2(\kappa T)^{s+2}} \int_0^\infty e^{-E/\kappa T} E^{s+1} \bar{Q}_n(E)\, \mathrm{d}E \qquad (4)$$

The factor $F(n, s)$ is defined in Ref. 6 and accounts for the normalization to the result for the scattering of unit hard spheres. The values of $\bar{\Omega}$ calculated from the $\bar{Q}_n$ of the present calculation, such as listed in Table 3, are contained in Tables 4 and 5 for C–C and C–N collisions, respectively. For N–N collisions at 100 K, the values of the diffusion integral $\bar{\Omega}_{1,1}(T)$ and the viscosity integral $\bar{\Omega}_{2,2}(T)$ are 11.42 Å^2 and 12.73 Å^2, respectively. The values of $\bar{\Omega}$ obtained for

Table 4 C–C collision integrals (Å²)

T, K	$\bar{\Omega}_{1,1}$	$\bar{\Omega}_{1,2}$	$\bar{\Omega}_{1,3}$	$\bar{\Omega}_{1,4}$	$\bar{\Omega}_{1,5}$	$\bar{\Omega}_{2,2}$	$\bar{\Omega}_{2,3}$	$\bar{\Omega}_{2,4}$	$\bar{\Omega}_{3,3}$
100	18.327	15.992	14.526	13.506	12.685	19.777	17.945	16.647	17.294
150	15.749	13.828	12.610	11.743	11.092	17.056	15.523	14.432	14.954
200	14.197	12.516	11.455	10.717	10.174	15.406	14.066	13.127	13.540
300	12.344	10.973	10.123	9.524	9.110	13.443	12.367	11.576	11.902
400	11.243	10.060	9.352	8.880	8.582	12.271	11.356	10.737	10.947
500	10.498	9.466	8.862	8.423	8.045	11.502	10.715	10.110	10.345
600	9.963	9.023	8.428	7.974	7.532	10.928	10.177	9.594	9.821
800	9.193	8.352	7.709	7.372	7.072	10.078	9.290	8.874	9.069
1,000	8.662	7.863	7.333	6.931	6.599	9.438	8.824	8.338	8.549
1,200	8.230	7.465	6.968	6.569	6.237	8.938	8.381	7.898	8.141
1,400	7.890	7.170	6.664	6.250	5.963	8.626	8.009	7.497	7.796
1,600	7.583	6.902	6.408	6.031	5.734	8.299	7.693	7.226	7.507
1,800	7.356	6.671	6.189	5.823	5.545	8.016	7.424	6.971	7.259
2,000	7.144	6.471	6.000	5.646	5.366	7.769	7.190	6.755	7.043
2,200	6.954	6.286	5.832	5.485	5.219	7.540	6.986	6.566	6.849
2,600	6.628	5.993	5.546	5.214	4.931	7.185	6.647	6.267	6.522
3,000	6.358	5.743	5.301	4.957	4.660	6.888	6.376	5.998	6.247
3,500	6.074	5.473	5.025	4.682	4.401	6.581	6.079	5.730	5.935
4,000	5.836	5.228	4.795	4.455	4.162	6.311	5.851	5.526	5.686
5,000	5.430	4.840	4.403	4.040	3.717	5.915	5.485	5.169	5.272
6,000	5.107	4.515	4.061	3.676	3.320	5.604	5.176	4.834	4.927
7,000	4.831	4.230	3.758	3.341	3.024	5.340	4.903	4.597	4.611
8,000	4.588	3.980	3.489	3.094	2.773	5.107	4.670	4.312	4.342
9,000	4.370	3.744	3.252	2.937	2.664	4.893	4.539	4.210	4.134
10,000	4.171	3.542	3.081	2.762	2.353	4.705	4.301	4.036	3.980
12,000	3.828	3.224	2.716	2.325	2.133	4.456	3.953	3.496	3.530
15,000	3.400	2.759	2.307	1.990	1.752	3.935	3.451	3.088	3.195
20,000	2.859	2.272	1.884	1.607	1.401	3.380	2.928	2.535	2.621
25,000	2.482	1.943	1.598	1.373	1.216	2.963	2.499	2.140	2.252
30,000	2.197	1.706	1.400	1.201	1.037	2.631	2.183	1.862	1.967

Table 5 C–N collision integrals (Å²)

T, K	$\bar{\Omega}_{1,1}$	$\bar{\Omega}_{1,2}$	$\bar{\Omega}_{1,3}$	$\bar{\Omega}_{1,4}$	$\bar{\Omega}_{1,5}$	$\bar{\Omega}_{2,2}$	$\bar{\Omega}_{2,3}$	$\bar{\Omega}_{2,4}$	$\bar{\Omega}_{3,3}$
100	15.085	12.744	11.176	10.107	9.299	16.240	14.659	13.447	13.631
150	12.452	10.485	9.277	8.498	7.977	13.739	12.262	11.176	11.404
200	10.892	9.248	8.301	7.713	7.307	12.137	10.842	9.959	10.126
300	9.172	7.956	7.291	6.864	6.581	10.305	9.327	8.680	8.745
400	8.233	7.270	6.760	6.456	6.263	9.279	8.518	8.057	8.004
500	7.647	6.863	6.474	6.236	6.082	8.667	8.075	7.702	7.599
600	7.254	6.598	6.252	6.056	5.862	8.327	7.731	7.413	7.314
800	6.750	6.233	5.955	5.785	5.684	7.698	7.256	6.985	6.896
1,000	6.427	6.000	5.761	5.573	5.384	7.333	6.959	6.682	6.641
1,200	6.206	5.823	5.572	5.337	5.110	7.064	6.695	6.387	6.409
1,400	6.032	5.661	5.388	5.121	4.917	6.833	6.458	6.128	6.191
1,600	5.884	5.511	5.214	4.964	4.749	6.631	6.244	5.938	5.989
1,800	5.751	5.371	5.063	4.816	4.617	6.451	6.066	5.767	5.818
2,000	5.629	5.243	4.939	4.689	4.495	6.290	5.911	5.618	5.673
2,200	5.519	5.108	4.820	4.578	4.399	6.131	5.775	5.494	5.542
2,600	5.321	4.925	4.622	4.398	4.207	5.902	5.553	5.285	5.326
2,800	5.232	4.834	4.537	4.310	4.107	5.800	5.455	5.202	5.229
3,000	5.149	4.756	4.459	4.226	4.029	5.711	5.366	5.115	5.145
3,500	4.959	4.574	4.270	4.044	3.862	5.498	5.174	4.943	4.943
4,000	4.807	4.407	4.119	3.895	3.701	5.328	5.030	4.817	4.790
5,000	4.539	4.150	3.866	3.628	3.389	5.074	4.801	4.597	4.546
6,000	4.325	3.932	3.646	3.356	3.089	4.872	4.600	4.350	4.316
7,000	4.141	3.736	3.408	3.105	2.889	4.695	4.396	4.129	4.095
8,000	3.979	3.571	3.218	2.936	2.698	4.531	4.230	3.981	3.909
9,000	3.829	3.395	3.049	2.764	2.517	4.388	4.081	3.822	3.746
10,000	3.687	3.248	2.898	2.617	2.353	4.257	3.942	3.672	3.598
12,000	3.442	2.989	2.627	2.327	2.072	4.020	3.685	3.391	3.330
15,000	3.133	2.661	2.292	1.983	1.758	3.708	3.342	3.024	2.991
20,000	2.721	2.241	1.881	1.621	1.427	3.269	2.876	2.548	2.558
25,000	2.403	1.937	1.616	1.386	1.229	2.915	2.523	2.207	2.247
30,000	2.155	1.711	1.431	1.223	1.087	2.629	2.260	1.949	2.017

N–N collisions at higher T are close to the corresponding tabulated results of our earlier calculations[6]; for example, the rms values of differences for the diffusion integral and the viscosity integral are only about 0.5 and 0.2%, respectively, for $T \leq 10{,}000$ K.

The uncertainty in the $\bar{\Omega}$ for interactions involving carbon arising from errors in the ab initio values of $V_i(r)$ is expected to be small because of the accuracy of the calculations described in Sec. II and the agreement of calculated and measured data shown in Tables 1 and 2. Furthermore, the major contribution to $\bar{\Omega}$ comes from the repulsive walls of the high-spin states at higher T (as just discussed); the small improvement in the N–N results obtained from the present studies also indicates that more accurate structure calculations for C–C and C–N will not yield values that are significantly different than those of Tables 4 and 5, respectively. Taking $2\Delta r/r$ as a rough estimate of uncertainty in the cross sections (and hence, $\bar{\Delta}\Omega/\bar{\Omega}$) and the rms value of the differences between the calculated and measured r_e of Table 1, we conclude that $\bar{\Delta}\Omega/\bar{\Omega}$ is only about 1%.

Convergence studies with decreasing increments in E of the numerical integration for Eq. (4), such as used for hydrogen atoms in Ref. 47, are impractical for the present work because of the large values of the atomic mass m; consequently, there can be small errors in the $\bar{\Omega}$ of Tables 4 and 5 that result from integrations with unresolved structure, which arises from resonance scattering[7,44] or other quantum mechanical effects.

From the preceding discussion about the relative contributions from the different states to $\bar{Q}_n(E)$ and Eq. (4), one concludes that the accuracy of the theoretical values of $\bar{\Omega}$ are heavily dependent on the accuracy of the ab initio calculations for excited states, especially at higher T. The diffusion and viscosity integrals of the present work agree fairly well with the corresponding results of Ref. 3 at lower T, but are smaller at higher T; the differences in the calculated values are only about 1% at 1000 K, but these differences rise with increasing T to about 17% at 25,000 K.

V. Comparison with Aufbau Approximations

With the exception of interactions involving rare-gas atoms, atom–atom transport properties have not been measured in the laboratory. Simplified approximations for the determination of atom–atom transport data are often based on inappropriate potential functions with parameters that are constructed from questionable empirical rules. On the other hand, the accurate theoretical determination of transport properties, such as just described, is a laborious procedure because it requires a complete set of interaction energies corresponding to all possible paths available to the collision. Studies are underway to develop simple Aufbau methods to estimate transport properties from effective atom–atom interaction energies $V_e(r)$ that are constructed from He–He and He–atom interaction energies. This approach is best suited to estimate transport data for repulsive interactions with a van der Waals minimum such as found for many molecular interactions. However, the simple modifications for interactions of atoms with electrons in the p shell as outlined next yields an effective method for scaling collision integrals such as those of nitrogen (because He–N interactions are described by a single potential energy curve) to estimate other atom–atom collision integrals.

This procedure requires the determination of accurate helium–atom energies. Partridge and Bauschlicher[48] have demonstrated that rapid convergence with respect to the size of the atom-centered basis sets can be achieved for weakly bound systems by adding bond functions. Consequently, the He–atom potential energies are obtained from a high-level computational method using composite wave functions. Specifically, a CCSD(T)[26,28] approach is combined with large aug-cc-pVQZ basis sets[14–16] and bond functions.[30] The energies are determined by the counterpoise method applied in Sec. III for nitrogen.

The construction of the atom–atom $V_e(r)$ is based on the following criteria. The leading long-range coefficient C_6 for He–atom interactions is obtained from the ab initio He–atom energy at large r; a required small contribution from the higher-order coefficients is estimated by the method outlined for carbon in Sec. II. The $V_{SR}(r)$ are extracted from the potential energies in the same manner[34] as used in Sec. III for nitrogen. For P state atoms the $V_{SR}(r)$ obtained for each of the two He–atom states are combined to construct an He–atom $V_e(r)$ that reproduces the He–atom $\bar{Q}_n(E)$ from accurate calculations. The atom–atom $V_e(r)$ is constructed (built up) from the $V_{SR}(r)$ and long-range interaction energies obtained using combination rules, for repulsive forces derived by Smith[49] and for C_6 established by Kramer and Herschbach,[50] respectively, and data for He–He and He–atom interactions.

Table 6 Comparison of log $(\bar{\Omega}/\bar{\Omega}_{N-N})$

Interaction	Aufbau	Diffusion	Viscosity
O–O	−0.03	−0.03[a]	−0.02[a]
C–C	0.13	0.13[b]	0.11[b]
B–B	0.19	0.22[c]	0.18[c]

[a]Ref. 6. [b]Table 4. [c]Ref. 40.

At higher T the collision integrals vary[51] as the square of a characteristic length scaling factor σ (which specifies the size of the interaction). Bzowski et al.[52] have shown that r_0 of the effective potential energy provides a satisfactory value for σ to achieve a correlation of experimental data. Bound state atom–atom interactions, however, differ from the van der Waals type of interactions studied in Ref. 52 in that an attractive electron exchange energy must be taken into account. The result of the additional contribution from the attractive regions of the potential is to extend the high-T slope of a plot of $\log\bar{\Omega}$ vs $\log T$ to include low T. The slopes for the carbon collision integrals found here at T in the range 300–3000 K is roughly the same as that found for other members[6,40] of the first row of the periodic chart that have electrons in the p valence shell. Hence, one expects that only the relative values of σ are required to explain the relative values of $\bar{\Omega}$ for different pairs of like-atom interactions.

The atom–atom $V_e(r)$ constructed from He interactions according to the criterion just outlined indicate, for example, that the $\bar{\Omega}$ for oxygen is about the same as that for nitrogen, but that the corresponding values for carbon are larger. Taking the values of r_0 to represent σ, one finds that the ratios $\sigma_{O-O}/\sigma_{N-N}$ and $\sigma_{C-C}/\sigma_{N-N}$ are 0.97 and 1.16, respectively. The values for the ratios of the collision integrals predicted from the preceding scaling arguments are compared in Table 6 with the corresponding results from tabulations of the diffusion and viscosity integrals at 3000 K. Similar comparisons are also shown for our boron results.[40] The comparisons of Table 6 confirm that a simple scaling procedure yields predictions for first-row transport properties that are comparable to our best results.

VI. Transport Properties

The values of $\bar{\Omega}_{1,2}$ and $\bar{\Omega}_{1,3}$ are required to determine the thermal conductivity of a binary mixture to first-order[51] in the Chapman–Cowling[53] expansion. Furthermore, the $\bar{\Omega}$ of Tables 4 and 5 allow transport properties to be calculated to second order if the collision integrals of existing formulations[51] are represented by the values obtained from Eq. (4). For example, the coefficient of viscosity for a pure gas is expressed in the form

$$\eta(T) = \frac{5}{16}\left(\frac{m\kappa T}{\pi}\right)^{\frac{1}{2}} \frac{f_\eta(T)}{\bar{\Omega}_{2,2}(T)} \tag{5}$$

the factor $f_\eta(T)$ can be calculated to second order[51] from the values of $\bar{\Omega}_{2,s}$ for $s = 2$–4. The first-order transport properties should be sufficient for most applications; the second-order contribution allows a test of the convergence of the Chapman–Cowling expansion for a particular transport property.

The $\eta(T)$ for C–C interactions obtained from a semiempirical estimate[54] for T in the range 2000–10,000 K are about 40–70% larger than the corresponding values obtained from Table 4.

The values of $\bar{\Omega}$ from the present calculation are applied to determine the transport properties of a gas composed of nitrogen and carbon atoms. Although such a gas might be difficult to produce or maintain in the laboratory, an examination of the transport behavior with composition leads to a better understanding of the role of these components in more complex gases or plasmas. We remove kinematical effects[46] to focus on the physics of the interaction. For

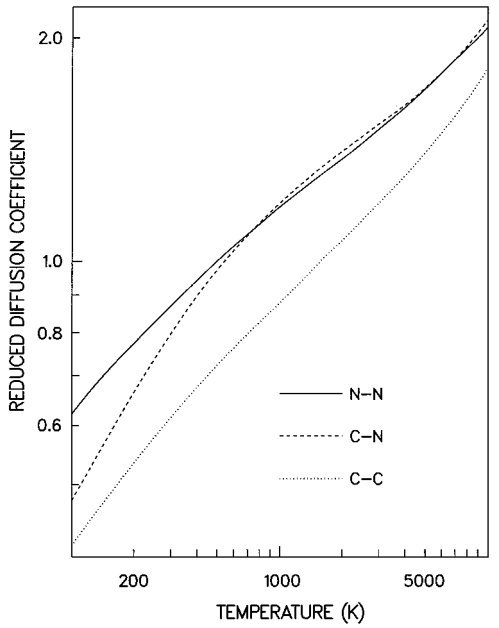

Fig. 3 Quantity pD^* at a pressure p of 1 atm as a function of temperature. The self-diffusion for nitrogen and carbon are shown by —— and ···· curves, respectively. The ---- curve for C–N binary diffusion is obtained for a 50/50 mixture (i.e., consisting of equal parts of carbon and nitrogen atoms).

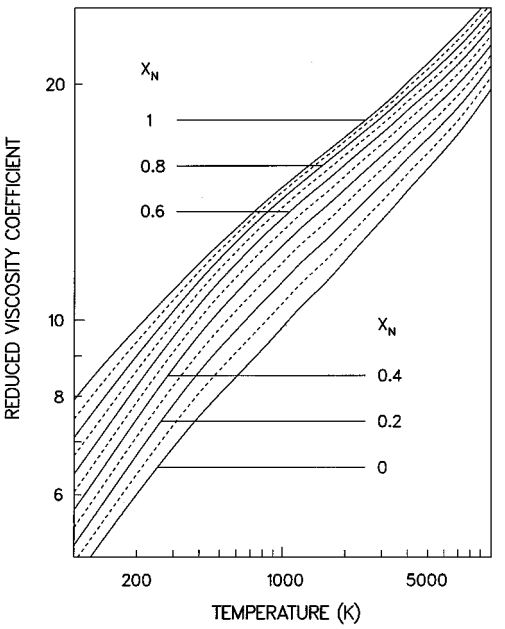

Fig. 4 Quantity η^* calculated to first order as a function of temperature for values of x_N specified by $N = n/10$ for integers n in the range 0–10. The η^* for even and odd values of n are represented by —— and ----, respectively.

convenience, we present our results using reduced transport coefficients. The binary (self for a pure gas) diffusion coefficient D in units of cm^2/s can be obtained from a reduced coefficient D^* defined by

$$pD^*(T) = 10^4 T^{-\frac{3}{2}} pD(T) = 26.287(2\mu)^{-\frac{1}{2}} \Big/ \bar{\Omega}_{1,1}(T) \quad (6)$$

similarly, the viscosity coefficient η in units of gm/(cm s) is obtained from

$$\eta^*(T) = 10^6 T^{-\frac{1}{2}} \eta(T) = 26.696(2\mu)^{\frac{1}{2}} \Big/ \bar{\Omega}_{2,2}(T) \quad (7)$$

where the reduced mass μ for the collision pair is in amu and $\bar{\Omega}$ is in $Å^2 = 10^{-16}$ cm^2. The physical constants required[51] for determining the coefficients of Eqs. (6) and (7) were taken from Cohen and Taylor.[55]

The curves for self-diffusion coefficients are compared with that for the binary coefficient in Fig. 3. The curve for the self-diffusion of carbon lies below the corresponding curve for nitrogen, as would be expected from comparisons of $\bar{Q}_1(E)$ in Table 3, and further, the curve for the binary diffusion coefficient is about the same as the self-diffusion curve for nitrogen at higher T.

The curves for viscosity are shown in Fig. 4 for various compositions specified by the molar fraction of nitrogen x_N, which ranges from 0 to 1 for a pure gas of carbon or nitrogen, respectively. The curve for viscosity rises monotonically for increasing x_N at constant T. Analogous to the binary self-diffusion similarity for collisions involving nitrogen, the C–N reduced[47] interaction viscosity[51] at higher T is closer to the value for a pure nitrogen gas than that for a pure carbon gas [as expected from a comparison of $\bar{Q}_2(E)$ from Table 3 for intermediate E]. This viscosity similarity can explain certain features of the curves; for example, it accounts for the large increase in $\log \eta^*$ at intermediate T around 1000 K when a small concentration of nitrogen is added to a carbon gas. Conversely, there is a relatively small decrease in $\log \eta^*$ when a small amount of carbon is added to a nitrogen gas.

The thermal diffusion factor α, which is a second-order effect, is shown in Fig. 5. Like the simple behavior of the curves for viscosity shown in Fig. 4, the curve for α also rises monotonically with increasing x_N at intermediate T around 2000 K; the variation of α with composition is large for intermediate T. Contrarily, the

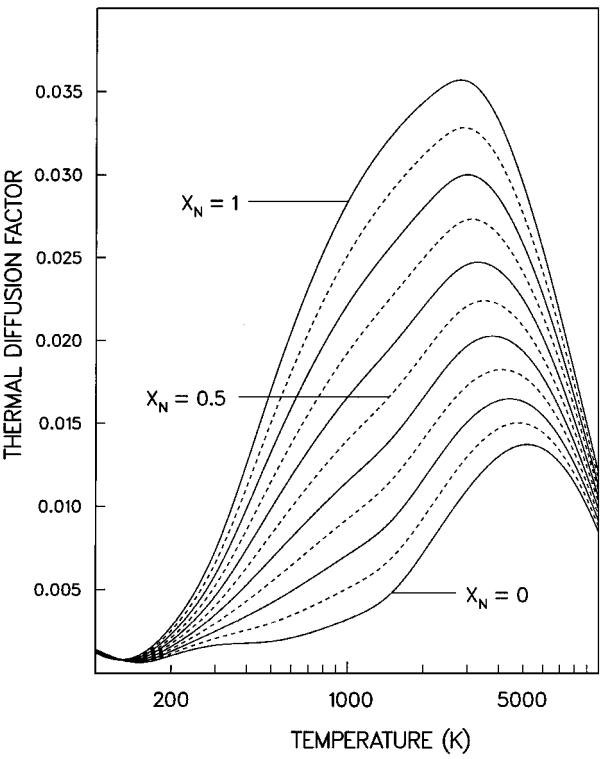

Fig. 5 Quantity α calculated to third order, which is the next order above the lowest order, as a function of temperature for the values of x_N that are specified and described for Fig. 4; for example, the curve for a 50/50 mixture (x_N = 0.5) is represented by a ----.

behavior of the curves for different compositions indicates that temperature inversions[46] occur at both small and large T.

The He–Ne potential energy has been calculated recently, using the high-level ab initio methods of Sec. III; the theoretical He–Ne transport coefficients are found to agree with the corresponding measured data[56] to within the experimental uncertainty. The theoretical atom–molecule diffusion coefficients[57,58] are in excellent agreement with the corresponding measured results. The accuracy that can be achieved with current ab initio methods as outlined in Secs. II and

III, the good agreement of the present theoretical spectroscopic constants with the measured data that is described in Sec. II, and the good agreement of the present values of $\bar{\Omega}$ for N–N discussed in Sec. IV indicate that the uncertainties in the $\bar{\Omega}$ of Tables 4 and 5 are small and consequently that the predicted transport properties are accurate.

VII. Conclusions

The potential energy curves for C–C and C–N interactions are determined from the results of accurate CI calculations. Potential energies of the high-spin states of N_2 are determined from experimental data and theoretical calculations. The potential data are applied to determine transport cross sections and collision integrals. The large temperature range for the tabulated collision integrals allows applications to studies for conditions with severe nonequilibrium. The results are further applied to verify that the excited states provide the dominant contribution to transport properties and, consequently, that an accurate determination of the atom–atom transport requires ab initio calculations of the potential energy curves. Small improvements in the potential energies are obtained for nitrogen; the present transport results are only slightly different than the corresponding N–N collision integrals of our earlier tabulation. The collision integrals for C–C indicate that the corresponding results of an earlier tabulation are too large and a more recent semiempirical estimate are too small at high temperatures.

From the discussion of Secs. IV and VI, we conclude that the $\bar{\Omega}$ of the present work for T above 300 K provide reliable data for transport studies. The present collision integrals are applied to study the variation of transport properties for mixtures of carbon and nitrogen atoms. The scattering results are also used to test the transport predictions from a simple Aufbau method. The Aufbau scaling factors are found to be an effective tool for estimating like-atom collision integrals at temperatures in the range 300–3000 K.

Acknowledgments

Support to Eugene Levin was provided by Contract NAS2-99092 from NASA to the Eloret Corporation. We thank David Schwenke for contributions to the manuscript.

References

[1]Meyyappan, M. (ed.), *Computational Modeling in Semiconductor Processing*, Artech House, Boston, 1995.

[2]Arnold, J. O., and Langhoff, S. R., "A Theoretical Study of the Electronic Transition Moment for the C_2 Swan Band System," *Journal of Quantitative Spectroscopy and Radiative Transfer,* Vol. 19, No. 5, 1978, pp. 461–466.

[3]Biolsi, L., Rainwater, R. C., and Holland, P. M., "Transport Properties of Monatomic Carbon," *Journal of Chemical Physics,* Vol. 77, No. 1, 1982, pp. 448–454.

[4]Fougere, F. P., and Nesbet, R. K., "Electronic Structure of C_2," *Journal of Chemical Physics,* Vol. 44, No. 1, 1966, pp. 285–298.

[5]Partridge, H., and Stallcop, J. R., "N^+–N and O^+–O Long-Range Interaction Energies and Resonance Charge Exchange," *Thermal Physical Aspects of Reentry Flows*, edited by J. N. Moss and C. D. Scott, Vol. 103, Progress in Astronautics and Aeronautics, AIAA, New York, 1986, pp. 243–260.

[6]Levin, E., Partridge, H., and Stallcop, J. R., "Collision Integrals and High Temperature Transport Properties for N–N, O–O, and N–O," *Journal of Thermophysics and Heat Transfer,* Vol. 4, No. 4, 1990, pp. 469–477.

[7]Stallcop, J. R., Partridge, H., and Levin, E., "Resonance Charge Transfer, Transport Cross Sections, and Collision Integrals for $N^+(^3P)$–$N(^4S^o)$ and $O^+(^4S^o)$–$O(^3P)$ Interactions," *Journal of Chemical Physics,* Vol. 95, No. 4, 1991, pp. 6429–6439.

[8]Urdahl, R. S., Bao, Y., and Jackson, W. M., "An Experimental Determination of the Heat of Formation of C_2 and the C–H Bond Dissociation Energy in C_2H," *Chemical Physics Letters,* Vol. 178, No. 4, 1991, pp. 425–428.

[9]Huang, Y., Barts, S. A., and Halpern, J. B., "Heat of Formation of the CN Radical," *Journal of Physical Chemistry,* Vol. 96, No. 1, 1992, pp. 425–428.

[10]Pradhan, A., Partridge, H., and Bauschlicher, C. W., "The Dissociation Energy of CN and C_2," *Journal of Chemical Physics,* Vol. 101, No. 5, 1994, pp. 3857–3861.

[11]Peterson, K. A., "Accurate Multireference Configuration Interaction Calculations on the Lowest $^1\Sigma^+$ and $^3\Pi$ Electronic States of C_2, CN^+, BN, and BO^+," *Journal of Chemical Physics,* Vol. 102, No. 1, 1995, pp. 262–277.

[12]Partridge, H., and Bauschlicher, C. W., "The Dissociation Energies of CH_4 and C_2H_2 Revisited," *Journal of Chemical Physics,* Vol. 103, No. 24, 1995, pp. 10,589–10,596.

[13]Peterson, K. A., Wilson, A. K., Woon, D. E., and Dunning, T. H., "Benchmark Calculations with Correlated Molecular Wave Functions. XII. Core Correlation Effects on the Homonuclear Diatomic Molecules B_2–F_2," *Theoretical Chemistry Accounts,* Vol. 97, No. 1–4, 1997, pp. 251–259.

[14]Dunning, T. H., "Gaussian Basis Sets for Use in Correlated Molecular Calculations. I. The Atoms Boron Through Neon and Hydrogen," *Journal of Chemical Physics,* Vol. 90, No. 2, 1989, pp. 1007–1023.

[15]Kendall, R. A., Dunning, T. H., and Harrison, R. J., "Electron Affinities of the First-Row Atoms Revisited. Systematic Basis Sets and Wave Functions," *Journal of Chemical Physics,* Vol. 96, No. 9, 1992, pp. 6796–6806.

[16]van Mourik, T., Wilson, A. K., and Dunning, T. H., "Benchmark Calculations with Correlated Molecular Wavefunctions. XIII. Potential Energy Curves for He_2, Ne_2, and Ar_2 Using Correlation Consistent Basis Sets Through Augmented Sextuple Zeta," *Molecular Physics,* Vol. 96, No. 4, 1999, pp. 529–547.

[17]Langhoff, S. R., and Davidson, E. R., "Configuration Interaction Calculations on the Nitrogen Molecule," *International Journal of Quantum Chemistry,* Vol. 8, No. 1, 1974, pp. 61–72.

[18]Bauschlicher, C. W., and Partridge, H., "Do Bond Functions Help for Calculation of Accurate Bond Energies?," *Journal of Chemical Physics,* Vol. 109, No. 12, 1998, pp. 4707–4712.

[19]Douay, M., Nietmann, R., and Bernath, P. F., "The Discovery of Two New Infrared Electronic Transitions of C_2: $B^1\Delta_g - A^1\Pi_u$ and $B'^1\Sigma_g^+ - A^1\Pi_u$," *Journal of Molecular Spectroscopy,* Vol. 131, No. 1, 1988, pp. 261–271.

[20]Huber, K. P., and Herzberg, G., *Molecular Spectra and Molecular Structure IV. Constants of Diatomic Molecules*, Reinhold, New York, 1979, pp. 112–114, 154.

[21]Chang, T. Y., "Moderately Long-Range Interatomic Forces," *Reviews of Modern Physics,* Vol. 39, No. 4, 1967, pp. 911–942.

[22]Desclaux, J. P., "Relativistic Dirac-Fock Expectation Values for Atoms with $Z = 1$ to $Z = 120$," *Atomic Data and Nuclear Data Tables,* Vol. 12, No. 4, 1973, pp. 311–359.

[23]Tang, K. T., and Toennies, J. P., "An Improved Simple Model for the van der Waals Potential Based on Universal Damping Functions for the Dispersion Coefficients," *Journal of Chemical Physics,* Vol. 80, No. 8, 1984, pp. 3726–3741.

[24]Starkshall, G., and Gordon, R. G., "Calculation of Coefficients in the Power Series Expansion of the Long-Range Dispersion Force Between Atoms," *Journal of Chemical Physics,* Vol. 56, No. 6, 1972, pp. 2801–2806.

[25]Bauschlicher, C. W., and Partridge, H., "How Large is the Effect of 1*s* Correlation on the D_e, ω_e and r_e of N_2?," *Journal of Chemical Physics,* Vol. 100, No. 7, 1994, pp. 4329–4335.

[26]Bartlett, R. J., "Many-Body Perturbation Theory and Coupled Cluster Theory for Electron Correlation in Molecules," *Annual Review of Physical Chemistry,* Vol. 32, 1981, pp. 359–401.

[27]Knowles, P. J., Hampel, C., and Werner, H.-J., "Coupled Cluster Theory for High Spin, Open Shell Reference Wave Functions," *Journal of Chemical Physics,* Vol. 99, No. 7, 1993, pp. 5219–5227.

[28]Raghavachari, K., Trucks, G. W., Pople, J. A., and Head-Gordon, M., "A Fifth-Order Perturbation Comparison of Electronic Correlation Theories," *Chemical Physics Letters,* Vol. 157, No. 6, 1989, pp. 479–483.

[29]Watts, J. D., Gauss, J., and Bartlett, R. J., "Coupled-Cluster Methods with Noniterative Triple Excitations for Restricted Open-Shell Hartree-Fock and Other General Simple Single Determinant Reference Functions. Energies and Analytical Gradients," *Journal of Chemical Physics,* Vol. 98, No. 11, 1993, pp. 8718–8733.

[30]Tao, F.-M., and Pan, Y.-K., "Møller-Plesset Perturbation Investigation of the He_2 Potential and the Role of Midbond Basis Functions," *Journal of Chemical Physics,* Vol. 97, No. 7, 1992, pp. 4989–4995.

[31]Boys, S. F., and Bernardi, F., "The Calculation of Small Molecular Interactions by the Differences of Separate Total Energies. Some Procedures with Reduced Errors," *Molecular Physics,* Vol. 19, No. 4, 1970, pp. 533–556.

[32]Partridge, H., Langhoff, S. R., and Bauschlicher, C. W., "Theoretical Study of the $^7\Sigma_u^+$ State of N_2," *Journal of Chemical Physics,* Vol. 84, No. 12, 1986, pp. 6901–6906.

[33]Stallcop, J. R., and Partridge, H., "The N_2–N_2 Potential Energy Surface," *Chemical Physics Letters,* Vol. 281, No. 1, 1997, pp. 212–220.

[34]Stallcop, J. R., Bauschlicher, C. W., Partridge, H., Langhoff, S. R., and Levin, E., "Theoretical Study of Hydrogen and Nitrogen Interactions: N–H Transport Cross Sections and Collision Integrals," *Journal of Chemical Physics,* Vol. 97, No. 8, 1992, pp. 5578–5585.

[35]Partridge, H., Langhoff S. R., Bauschlicher, C. W., and Schwenke, D. W., "Theoretical Study of the $A'^5\Sigma_g^+$ and $C'^5\Pi_u$ States of N_2: Implication for the N_2 Afterglow," *Journal of Chemical Physics,* Vol. 88, No. 5, 1988, pp. 3174–3186.

[36]Huber, K. P., and Vervloet, M., "High-Resolution Fourier Transform Spectroscopy of Supersonic Jets. The $C'^5\Pi_{ui} \rightarrow A'^5\Sigma_g^+$ Herman Infrared Bands of $^{14}N_2$," *Journal of Molecular Spectroscopy,* Vol. 153, No. 1, 1992, pp. 17–25.

[37] Ottlinger, C., and Vilesov, A. F., "Laser Spectroscopy of Perturbed Levels in $N_2(A'^5\Sigma_g^+)$ Term Energy," *Journal of Chemical Physics,* Vol. 100, 1994, No. 7, pp. 4862–4869.

[38] Hickman, A. P., Medikeri-Naphade, M., Chapin, C. D., and Huestis, D. L., "Calculation of Fine-Structure Effects in O^+–O Collisions," *Physical Review A,* Vol. 56, No. 6, 1997, pp. 4633–4643.

[39] Cohen, J. S., and Schneider, B., "Ground and Excited States of Ne_2 and Ne_2^+. I. Potential Curves with and Without Spin-Orbit Coupling," *Journal of Chemical Physics,* Vol. 61, No. 8, 1974, pp. 3230–3238.

[40] Levin, E., Stallcop, J. R., and Partridge, H., "Transport Properties of Boron and Aluminum," *Theoretical Chemistry Accounts*, Vol. 103, No. 6, 2000, pp. 518–523.

[41] Smith, F. J., "Low Energy Elastic and Resonant Exchange Cross Sections Between Complex Atoms," *Molecular Physics,* Vol. 13, No. 2, 1967, pp. 121–130.

[42] Mason, E. A., Vanderslice, J. T., and Yos, J. M., "Transport Properties of High-Temperature Multicomponent Gas Mixtures," *Physics of Fluids,* Vol. 2, No. 6, 1959, pp. 688–694.

[43] Levin, E., Schwenke, D. W., Stallcop, J. R., and Partridge, H., "Comparison of Semiclassical and Quantum Mechanical Methods for the Determination of Transport Cross Sections," *Chemical Physics Letters,* Vol. 227, No. 1, 1994, pp. 669–675.

[44] Stallcop, J. R., Partridge, H., and Levin, E., "Potential Energies and Collision Integrals for the Interactions of Air Components. II. Scattering Calculations and Interactions Involving Ions," *Molecular Physics and Hypersonic Flows*, edited by M. Capitelli, Kluwer Academic, Norwell, MA, 1996, pp. 339–349.

[45] Yun, K. S., and Mason, E. A., "Collision Integrals for the Transport Properties of Dissociating Air at High Temperatures," *Physics of Fluids,* Vol. 5, No. 4, 1962, pp. 380–386.

[46] Hirschfelder, J. O., Curtiss, C. F., and Bird, R. B., *Molecular Theory of Gases and Liquids*, Wiley-Interscience, New York, 1964, p. 526.

[47] Stallcop, J. R., Partridge, H., and Levin, E., "Transport Properties of Hydrogen," *Journal of Thermophysics and Heat Transfer,* Vol. 4, No. 4, 1998, pp. 514–519.

[48] Partridge, H., and Bauschlicher, C. W., "The Dissociation Energies of He_2, HeH, and ArH: a Bond Function Study," *Molecular Physics,* Vol. 96, No. 4, 1999, pp. 705–710.

[49] Smith, F. T., "Atomic Distortion and the Combining Rule for Repulsive Potentials," *Physical Review A,* Vol. 5, No. 4, 1972, pp. 1708–1713.

[50] Kramer, H. L., and Herschbach, D. R., "Combination Rules for van der Waals Force Constants," *Journal of Chemical Physics,* Vol. 53, No. 7, 1970, pp. 2792–2800.

[51] Maitland, G. C., Rigby, M., Smith, E. B., and Wakeham, W. A., *Intermolecular Forces. Their Origin and Determination*, Oxford Univ., Oxford, 1981, pp. 297, 298.

[52] Bzowski, J., Kestin, J., Mason, E. A., and Uribe, F. J., "Equilibrium and Transport Properties of Gas Mixtures at Low Density: Eleven Polyatomic Gases and Five Noble Gases," *Journal of Physical and Chemical Reference Data,* Vol. 19, No. 5, 1990, pp. 1179–1232.

[53] Chapman, S., and Cowling T. G., *The Mathematical Theory of Non-Uniform Gases*, 3rd ed., Cambridge Univ. Press, New York, 1970.

[54] Riabov, V. V., "Approximate Calculation of Transport Coefficients of the Earth and Mars Atmospheric Dissociating Gases," *Journal of Thermophysics and Heat Transfer*, Vol. 10, No. 2, 1995, pp. 209–216.

[55] Cohen, E. R., and Taylor, B. N., "The 1986 CODATA Recommended Values of the Fundamental Physical Constants," *Journal of Physical and Chemical Reference Data*, Vol. 17, No. 4, 1988, pp. 1795–1803.

[56] Keil, M., Danielson, L. J., Buck, U., Schleusener, J, Huisken, F., and Dingle, T. W., "The HeNe Interatomic Potential from Multiproperty Fits and Hartree-Fock Calculations," *Journal of Chemical Physics,* Vol. 89, No. 5, 1988, pp. 2866–2880.

[57] Stallcop, J. R., Partridge, H., Walch, S. P., and Levin, E., "H–N_2 Interaction Energies, Transport Cross Sections, and Collision Integrals," *Journal of Chemical Physics,* Vol. 97, No. 5, 1992, pp. 3431–3436.

[58] Stallcop, J. R., Partridge, H., and Levin, E., "H–H_2 Collision Integrals and Transport Coefficients," *Chemical Physics Letters,* Vol. 254, No. 1, 1996, pp. 301–307.